Loschmidt echo in one-dimensional interacting Bose gases

Lelas, Karlo; Ševa, Tomislav; Buljan, Hrvoje

Source / Izvornik: **Physical Review A, 2011, 84**

Journal article, Published version
Rad u časopisu, Objavljena verzija rada (izdavačev PDF)

https://doi.org/10.1103/PhysRevA.84.063601

Permanent link / Trajna poveznica: https://urn.nsk.hr/urn:nbn:hr:217:877943

Rights / Prava: In copyright / Zaštićeno autorskim pravom.

Download date / Datum preuzimanja: **2024-03-29**

Repository / Repozitorij:

Repository of the Faculty of Science - University of Zagreb

Loschmidt echo in one-dimensional interacting Bose gases

K. Lelas*
Faculty of Electrical Engineering Mechanical Engineering and Naval Architecture, University of Split, Rudjera Boškovića BB, 21000 Split, Croatia

T. Ševa† and H. Buljan‡
Department of Physics, University of Zagreb, Bijenička c. 32, 10000 Zagreb, Croatia
(Received 12 April 2011; published 2 December 2011)

We explore Loschmidt echo in two regimes of one-dimensional interacting Bose gases: the strongly interacting Tonks-Girardeau (TG) regime, and the weakly interacting mean-field regime. We find that the Loschmidt echo of a TG gas decays as a Gaussian when small (random and time independent) perturbations are added to the Hamiltonian. The exponent is proportional to the number of particles and the magnitude of a small perturbation squared. In the mean-field regime the Loschmidt echo shows richer behavior: it decays faster for larger nonlinearity, and the decay becomes more abrupt as the nonlinearity increases; it can be very sensitive to the particular realization of the noise potential, especially for relatively small nonlinearities.

DOI: 10.1103/PhysRevA.84.063601 PACS number(s): 03.75.Kk, 05.30.−d, 03.65.Yz, 67.85.De

I. INTRODUCTION

The understanding of why an isolated (interacting many-body) system, which is initially, say, far from equilibrium, in many cases macroscopically undergoes irreversible evolution toward an equilibrium state, despite the fact that the microscopic laws are reversible, has intrigued scientists ever since the first disputes between Boltzmann and Loschmidt on this topic [1,2]. In principle, if the time was reversed at a given instance, the system would evolve back into the initial state. However, such a reversal is for all practical purposes impossible due to high sensitivity to small errors and the interaction of the system with the environment. The quantity that measures the sensitivity of quantum motion to perturbations is called the *Loschmidt echo* or *fidelity* [3–7] (for a review see, e.g., Ref. [8]). The Loschmidt echo tells us the probability that system will end up in the initial state after forward evolution for time t, followed by the slightly imperfect time-reversed evolution for the same time t. In quantum mechanics time evolution from an initial state ψ_0 is given by the unitary operator $\hat{U}(t) = \exp(-i\hat{H}t/\hbar)$ via $\psi(t) = \exp(-i\hat{H}t/\hbar)\psi_0$, and the echo dynamics can be formally written as

$$F(t) = |\langle\psi_0|\exp(i\hat{H}'t/\hbar)\exp(-i\hat{H}t/\hbar)|\psi_0\rangle|^2. \quad (1)$$

Here $\hat{H}$ is the Hamiltonian of the unperturbed system, and $\hat{H}' = \hat{H} + \hat{V}_\varepsilon$ is the slightly perturbed Hamiltonian [8]. We emphasize that the Loschmidt echo and the fidelity are two names for the same concept. One can think about $F(t)$ as measuring the stability of quantum motion [3]; i.e., it tells us the overlap of the two states $\psi(t)$ and $\psi'(t)$, the former evolved forward in time by $\hat{H}$, and the latter by $\hat{H}'$:

$$F(t) = |\langle\psi'(t)|\psi(t)\rangle|^2. \quad (2)$$

In quantum systems, depending on the strength of the perturbation and the properties of the nonperturbed Hamiltonian, three different decay regimes of Loschmidt echo are usually identified: the Gaussian perturbative regime [5,6], the exponential Fermi golden rule regime [4–7] and the Lyapunov regime [4].

Motivated by the recent progress in experiments and theory on ultracold atomic gases [9], where the influence of the environment can be made very small and the strength of the atom-atom interactions can be tuned [9], we are motivated to investigate Loschmidt echo dynamics in those systems. In particular, we focus on one-dimensional (1D) Bose gases which were experimentally realized [10] even in the strongly correlated regime of Tonks-Girardeau (TG) bosons [11,12], both in and out of equilibrium [11,12]. The realization of the TG gas in atomic waveguides was proposed by Olshanii [13]. The 1D atomic gases can be described with the Lieb-Liniger model [14], where dynamics can for weak interactions be approximated by the mean-field theory [9] (nonlinear Schrödinger equation in the Gross-Pitaevskii approximation), whereas for sufficiently strong interactions one enters the Tonks-Girardeau regime, where exact solutions can be found via Fermi-Bose mapping [15]. This method was used to study out-of-equilibrium dynamics in the strongly correlated regime (e.g., see Refs. [16–21]). We use the two methods, the mean-field theory and the Fermi-Bose mapping, to study Loschmidt echo dynamics in the weakly and strongly interacting regimes (respectively) of 1D gases.

The experiments on Loschmidt echo dynamics with ultracold atoms, for example in atom-optics billiards [22], have mostly considered single-particle dynamics. However, this quantity is also related to a series of experiments [23–25] and theoretical papers [26–31] on interference between parallel quantum-degenerate interacting 1D Bose systems. More specifically, if a 1D quasicondensate is phase-coherently split along the axial direction (x in this paper), and then held for some holdup time after which all potentials (including the transverse ones) are turned off, the quasicondensates will interfere [23–25]. The interference pattern contains information on the dynamics of coherence, and in fact such experiments

*klelas@fesb.hr
†tseva@phy.hr
‡hbuljan@phy.hr

 ©2011 American Physical Society

can be used to measure the dynamics of the Loschmidt echo. The measured subexponential decay of the coherence factor in Ref. [23] (which is related to fidelity) was predicted by using Luttinger liquid theory [29]; the same functional form but with different scaling of the characteristic time is found in Refs. [30,31].

In this paper we focus on a decay of fidelity due to small external spatial noise in the system, and we assume that the temperature is zero. The motivation for studying this type of noise is twofold: (i) it is of theoretical interest to understand the reversibility of the dynamics in disordered potentials, where intriguing phenomena such as Anderson localizations occur [32], and (ii) such time-independent spatially varying noise can be present in experiments (e.g., it is designed by using optical speckle potentials [32] and they are found in atom-chip systems for small trap-surface distances; see Ref. [25]). The Loschmidt echo was for a small time-independent noise potential addressed within the mean-field Gross-Pitaevskii theory in Ref. [33], and in a kicked optical lattice in Ref. [34]. We would also like to point out studies of orthogonality catastrophe (and the relation to Loschmidt echo) in an ultracold Fermi gas coupled to a single cubit [35], and long-time behavior of many-particle quantum decay [36]. Fidelity decay in the k-body embedded ensembles of random matrices for bosons distributed in two single-particle states, where the mean-field approach was the unperturbed Hamiltonian and residual interaction the perturbation, was studied in Ref. [37].

Here we demonstrate, with exact numerical calculation, that for small spatially random time-independent perturbation, the Loschmidt echo (i.e., fidelity) for a TG gas decays as a Gaussian with decay constant proportional to the number of particles and the square of the amplitude of the perturbation. We analytically derive the Gaussian behavior of TG fidelity within the approximation presented by Peres [3]. In the mean-field regime the Loschmidt echo decays faster for larger nonlinearity, and for larger linear densities the decay becomes more abrupt [33]; it can be very sensitive to the particular realization of the noise potential, especially for relatively small nonlinearities. Finally, we discuss the relation of the Loschmidt echo dynamics studied here to the already existing experiments, and propose further measurements.

II. THE PHYSICAL SYSTEM AND THE CORRESPONDING MODEL

Consider a gas of N identical bosons in a 1D space, which interact via pointlike interactions, described by the Hamiltonian

$$H=\sum_{i=1}^{N}\left[-\frac{\hbar^2}{2m}\frac{\partial^2}{\partial X_i^2}+U(X_i)\right]+g_{1\mathrm{D}}\sum_{1\leqslant i<j\leqslant N}\delta(X_i-X_j). \tag{3}$$

Such a system can be realized with ultracold bosonic atoms trapped in effectively 1D atomic waveguides [10–12], where $U(X)$ is the axial trapping potential, and $g_{1\mathrm{D}}=2\hbar^2 a_{3\mathrm{D}}[ma_\perp^2(1-Ca_{3\mathrm{D}}/\sqrt{2}a_\perp)]^{-1}$ is the effective 1D coupling strength; $a_{3\mathrm{D}}$ stands for the three-dimensional s-wave scattering length, $a_\perp=\sqrt{\hbar/m\omega_\perp}$ is the transverse width of the trap, and $C=1.4603$ [13]. By varying say $\omega_\perp$, the system can be tuned from the mean-field regime described by the Gross-Pitaevskii equation up to the strongly interacting Tonks-Girardeau regime ($g_{1\mathrm{D}}\to\infty$). In equilibrium, different regimes of these 1D gases are usually characterized by a dimensionless parameter $\gamma=mg_{1\mathrm{D}}/\hbar^2 n_{1\mathrm{D}}$, where $n_{1\mathrm{D}}$ stands for the linear atomic density. For $\gamma\ll 1$ the gas is in the mean-field regime and for $\gamma\gg 1$ it is in the strongly interacting regime (we consider repulsive interactions $\gamma>0$) [11–14]. In our calculations, we use Hamiltonian (3) in its dimensionless form,

$$H=\sum_{i=1}^{N}\left[-\frac{\partial^2}{\partial x_i^2}+V(x_i)\right]+2c\sum_{i<j}^{N}\delta(x_i-x_j), \tag{4}$$

where $x=X/X_0$ (X_0 is the spatial scale which we choose to be 1 μm). Here we consider ^{87}Rb atoms with the 3D scattering length $a_{3\mathrm{D}}=5.3$ nm [11,12]. Energy is in units of $E_0=\hbar^2/2mX_0^2=3.82\times10^{-32}$ J, and time is in units of $T_0=2mX_0^2/\hbar=2.8$ ms. The dimensionless axial potential is $V(x)=U(X)/E_0$, and the interaction strength parameter is $2c=g_{1\mathrm{D}}/X_0E_0$.

III. LOSCHMIDT ECHO OF A TONKS-GIRARDEAU GAS

For the Tonks-Girardeau gas, the interaction strength is infinite ($c\to\infty$); that is, the bosons are "impenetrable" [15]. Consequently, an exact (static and time-dependent) solution of this model can be written via Girardeau's Fermi-Bose mapping [15,16]

$$\psi_B(x_1,\ldots,x_N,t)=\prod_{1\leqslant i<j\leqslant N}\mathrm{sgn}(x_i-x_j)\psi_F(x_1,\ldots,x_N,t), \tag{5}$$

where ψ_F denotes a wave function describing N noninteracting spin-polarized fermions in the external potential $V(x)$. In our simulations we consider up to $N=70$ particles. The system is initially (for times $t\leqslant 0$) in the ground state of a containerlike potential,

$$V_L(x)=V_0\{1+\tanh[V_s(x-L/2)]/2-\tanh[V_s(x+L/2)]/2\}, \tag{6}$$

where $V_0=500$, $V_s=4$, and $L=15$ (corresponding to 15 μm). At $t=0$ we suddenly expand the width of the container to twice its original width; that is, the potential at time $t>0$ is $V_{2L}(x)$. In order to calculate the fidelity $F(t)$, we must evolve the TG gas in the new potential $V_{2L}(x)$, and in the potential $V'_{2L}(x)=V_{2L}(x)+V_\varepsilon(x)$ starting from identical initial states. Here $V_\varepsilon(x)$ is a small noise potential of amplitude ε. The Loschmidt echo $F(t)=|\langle\psi'_B(t)|\psi_B(t)\rangle|^2$ is calculated from the knowledge of the TG many-body states $\psi_B(t)$ and $\psi'_B(t)$ corresponding to the evolution in potentials $V_{2L}(x)$ and $V'_{2L}(x)$, respectively.

The fermionic wave function ψ_F can in our case be written as a Slater determinant, $\psi_F(x_1,\ldots,x_N,t)=\det_{m,n=1}^{N}[\psi_m(x_n,t)]/\sqrt{N!}$, where $\psi_m(x,t)$, $m=1,\ldots,N$, satisfy the single-particle Schrödinger equation

$$i\frac{\partial\psi_m(x,t)}{\partial t}=\left[-\frac{\partial^2}{\partial x^2}+V_{2L}(x)\right]\psi_m(x,t), \tag{7}$$

and equivalently for $\psi_m^{'}(x,t)$ which evolve in $V_{2L}'(x)$. The initial conditions are such that $\psi_m(x,0) = \psi_m^{'}(x,0)$ is the mth single-particle eigenstate of the initial container potential $V_L(x)$. The Loschmidt echo for a Tonks-Girardeau gas can be written in a form convenient for calculation:

$$\begin{aligned}|\langle\psi_B'(t)|\psi_B(t)\rangle|^2 &= \left|\frac{1}{N!}\int dx_1\cdots dx_N\right.\\ &\quad\times\sum_{\sigma_1}(-)^{\sigma_1}\prod_{i=1}^{N}\psi_{\sigma_1(i)}^{'*}(x_i,t)\\ &\quad\left.\times\sum_{\sigma_2}(-)^{\sigma_2}\prod_{j=1}^{N}\psi_{\sigma_2(j)}(x_j,t)\right|^2\\ &= \left|\frac{1}{N!}\sum_{\sigma_1}\sum_{\sigma_2}(-)^{\sigma_1}(-)^{\sigma_2}\prod_{i=1}^{N}P_{\sigma_1(i)\sigma_2(i)}(t)\right|^2\\ &= |\det\mathbf{P}(t)|^2, \end{aligned}\tag{8}$$

where σ denotes a permutation in N indices, $(-)^{\sigma}$ is its signature, and

$$P_{ij}(t) = \int \psi_i^{'*}(x,t)\psi_j(x,t)dx. \tag{9}$$

In writing relation (8) we used a definition of the determinant. Since at $t = 0$ we have $P_{ij}(0) = \delta_{ij}$, that motivates us to define the fidelity product

$$F_P(t) = \prod_{i=1}^{N} P_{ii}(t)P_{ii}^*(t). \tag{10}$$

Thus, in calculation of the fidelity product we assume that all off-diagonal elements of the matrix (9) are zero; i.e., $P_{ij}(t) = 0$ for $i \neq j$ for all times. It can be interpreted as if we evolve the N particles fully independently of each other (including statistics) starting from the N initial states $\psi_m(x,0)$, $m = 1,\ldots,N$, calculate N different fidelities for these states, and multiply them to obtain the product fidelity. The value $F(t)$ is identical for noninteracting spinless fermions and interacting TG bosons; note that Eq. (8) is *identical* to the formula used by Goold *et al.* [35] studying the orthogonality catastrophe for ultracold fermions. Thus, F_P and F will distinguish the influence of antisymmetrization in the case of noninteracting fermions, or TG interactions and symmetrization in the case of bosons, with dynamics which takes neither statistics nor interactions into account. We would like to emphasize that derivation of Eqs. (8) and (9) does not require that we initiate the dynamics from the ground state of the TG gas in the initial trap; we could have chosen any excited TG eigenstate as an initial condition as well.

In order to calculate the fidelity $F(t)$, we must evolve the single-particle states $\psi_j(x,t)$ [$\psi_j^{'}(x,t)$, respectively], in the potential $V_{2L}(x)$ [$V_{2L}(x) + V_\varepsilon(x)$], starting from the first N single-particle eigenstates of $V_L(x)$. The evolution is performed via standard linear superposition in terms of the eigenstates $\phi_m(x)$ of the final container potential $V_{2L}(x)$ (which are calculated numerically):

$$\psi_j(x,t) = \sum_m a_m^j\phi_m(x)\exp(-iE_mt) \tag{11}$$

and

$$\psi_j'(x,t) = \sum_m a_m^{j'}\phi_m'(x)\exp(-iE_m't). \tag{12}$$

We numerically calculate the coefficients $a_n^{j'} = \int\phi_m^{'*}(x)\psi_j(x,0)dx$ and $a_n^j = \int\phi_m^*(x)\psi_j(x,0)dx$ for $j = 1,\ldots,70$, and $m = 1,\ldots,210$, which is sufficient for the parameters we used. The noise potential is constructed as follows: x space is numerically simulated by using 2048 equidistant points in the interval $x \in [-30,30]$. From this array we construct a random array $V_{\rm rand}(x) = |FT^{-1}\{\exp(-k^4/K_{\rm cut}^4)FT[{\rm rand}(x)]\}|$ of the same length, where rand(x) is a random number between 0 and 1, FT stands for the Fourier transform, and $K_{\rm cut}$ is the cutoff wave vector (set to $K_{\rm cut} = 53$) introduced to make the discrete numerical potential sufficiently "smooth" from point to point. Finally the noise potential is obtained via $V_\varepsilon(x) = \varepsilon[V_{\rm rand}(x) - \bar{V}_{\rm rand}]$, where ε is the amplitude of the perturbation, and $\bar{V}_{\rm rand}$ is the mean value of $V_{\rm rand}(x)$. Such a potential can be constructed optically for 1D Bose gases [32].

The fidelity depends on the particle number N and the amplitude of noise, ε, but also on the particular realization of $V_\varepsilon(x)$; hence, we calculate all quantities (e.g., the Loschmidt echo) for 50 different realizations of $V_\varepsilon(x)$ and then perform the average over the noise ensemble: $\langle F(t)\rangle_{\rm noise}$.

In Fig. 1(a) we show the fidelity $\langle F(t)\rangle_{\rm noise}$ as a function of time for three different numbers of particles, $N = 10$, 20, and 50, with $\varepsilon = 0.05$. We find that in the TG regime, the Loschmidt echo decays as a Gaussian: $\langle F(t)\rangle_{\rm noise} = \exp(-\langle\lambda(N,\varepsilon)\rangle t^2)$; solid black lines represent the Gaussian curves fitted to the numerically obtained values. We point out that in every single realization of the noise, the fidelity for a TG gas decays as a Gaussian, with small fluctuations in the value of the exponent. The error bars in Fig. 1(a) represent the standard deviation of the fidelity at a given time. Note that the standard deviation gets smaller with increasing particle number N, which means that for sufficiently large N it suffices to calculate the fidelity decay for a single realization of the potential to obtain reliable values for $\lambda(N,\varepsilon)$. It is interesting to compare the fidelity with the fidelity product $\langle F_P(t)\rangle_{\rm noise}$, which can also be fitted well with the Gaussian function as illustrated in Fig. 1(b). We find that the product $\langle F_P(t)\rangle_{\rm noise}$ is systematically below the value of the fidelity.

In Fig. 2 we depict the dependence of the fidelity, that is, of the exponent $\langle\lambda(N,\varepsilon)\rangle$, on the number of particles N and ε. In Fig. 2(a) we plot $\langle\lambda(N,\varepsilon)\rangle/\varepsilon^2$ as a function of ε for different values of N; evidently we have $\langle\lambda(N,\varepsilon)\rangle \propto \varepsilon^2$. In Fig. 2(b) we plot $\langle\lambda(N,\varepsilon)\rangle/N$ as a function of N for $\varepsilon = 0.05$; we clearly see that $\langle\lambda(N,\varepsilon)\rangle \propto N$ for sufficiently large N (already for $N > 20$).

In order to understand numerical results of Figs. 1 and 2, we analytically explore the properties of the fidelity for a single realization of $V_\varepsilon(x)$. To this end we use an approximation from Peres [3], where to first order in ε one has $\int dx\phi_j^{'*}\phi_i \approx \delta_{ij}$, and $a_m^j \approx a_m^{j'}$. The elements of the matrix $\mathbf{P}$, which yield the fidelity via Eq. (8), are then written as $P_{ij} = \sum_n a_n^{i*}a_n^j\exp(i\omega_nt)$, where $\omega_n = E_n' - E_n \approx \langle\phi_n|V_\varepsilon|\phi_n\rangle$. In Fig. 1(b) we plot the fidelity obtained with this approximation (solid blue line) and the one obtained with the exact numerical evolution

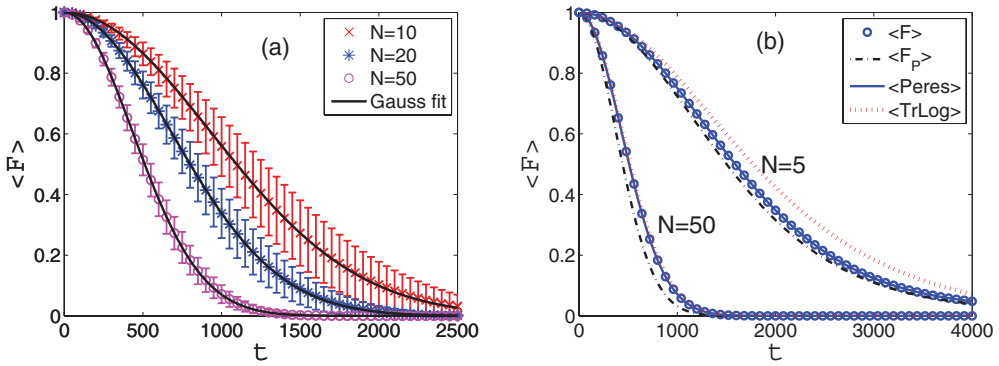


FIG. 1. (Color online) Decay of the Loschmidt echo (fidelity) with time for $\varepsilon = 0.05$. (a) The averaged values $\langle F(t)\rangle_{\text{noise}}$ for $N = 10$ (crosses), $N = 20$ (asterisks), and $N = 50$ (circles). Solid black lines represent the Gaussian functions fitted to the numerically obtained values. Error bars depict the standard deviation for 50 different realizations of the noise potential $V_\varepsilon(x)$. (b) The fidelity $\langle F(t)\rangle_{\text{noise}}$ (circles), fidelity product $\langle F_P(t)\rangle_{\text{noise}}$ (black dot-dashed lines), the values obtained via $\det(\mathbf{PP}^\dagger)$, where $P_{ij} = \sum_n a_n^{i*} a_n^j \exp(i\omega_n t)$ is obtained via approximation presented by Peres [3] [solid (blue) line], and the fidelity obtained via trace-log formula Eq. (14) [dotted (red) line].

(blue circles); the agreement is excellent. The diagonal elements $|P_{ii}(t)|^2$ can be interpreted as single-particle fidelities corresponding to the initial states $\psi_i(x,0)$. It is straightforward to see that $|P_{ii}(t)|^2 = \sum_{n,m} |a_n^i|^2 |a_m^i|^2 \cos[(\omega_n - \omega_m)t]$; however, we note that in our simulations only a few terms contribute to the sum above, yielding oscillatory behavior of the single-particle fidelities with relatively high amplitudes of the oscillation. Now we turn to the TG gas and our observation that the decay of fidelity is Gaussian. In order to derive this we use the trace-log formula for the determinants:

$$F(t) = \exp\{\mathrm{Tr}[\ln(\mathbf{PP}^\dagger)]\}. \tag{13}$$

We can approximate $\mathbf{PP}^\dagger \approx \mathbf{1} + \mathbf{Q_1} t - \mathbf{Q_2} t^2 + O(t^3)$, where $\Delta_{nm} = \omega_n - \omega_m$, $\quad [Q_1]_{ij} = i \sum_{k=1}^N \sum_{n,m} a_n^{i*} a_n^k a_m^j a_m^{k*} \Delta_{nm}$, and $[Q_2]_{ij} = \frac{1}{2} \sum_{k=1}^N \sum_{n,m} a_n^{i*} a_n^k a_m^j a_m^{k*} \Delta_{nm}^2$. Next we expand the logarithm in trace-log formula, which yields

$$F(t) = \exp(-\mathrm{Tr}\mathbf{Q_2} t^2), \tag{14}$$

i.e., a Gaussian function. In our derivation we used $\mathrm{Tr}\mathbf{Q_1} = 0$. The (red) dotted line in Fig. 1(b) shows that Eq. (14) is an excellent approximation for larger N. The dependence of $\langle\lambda(N,\varepsilon)\rangle$ on ε follows from the fact that $\Delta_{nm}^2 \propto \varepsilon^2$, whereas $\mathrm{Tr}\mathbf{Q_2} \propto N$ (see Fig. 2).

In the rest of this section we argue that $F_P(t) < F(t)$, i.e., that the fidelity product is smaller than the fidelity. Obviously we need only diagonal elements of the matrix $\mathbf{PP}^\dagger$ to construct either $F(t)$ or $F_P(t)$, which we write as

$$(\mathbf{PP}^\dagger)_{ii} = |P_{ii}(t)|^2 + \sum_{k=1, k\neq i}^{N} |P_{ik}(t)|^2. \tag{15}$$

For the first term we can write $|P_{ii}(t)|^2 = 1 - \alpha_i(t)$, where $\alpha_i(t)$ is some function of time with properties $\alpha_i(0) = 0$ and $0 \leqslant \alpha_i(t) \leqslant 1$ due to relation (9). For the second term we write $\sum_{k=1,k\neq i}^N |P_{ik}(t)|^2 = \beta_i(t)$, where $\beta_i(0) = 0$ and $\beta_i(t) \geqslant 0$. It follows that $(\mathbf{PP}^\dagger)_{ii} = 1 - [\alpha_i(t) - \beta_i(t)]$. By applying the trace-log formula in the same manner as before, we get for the fidelity $F(t) = \exp[-\sum_{i=1}^N \alpha_i(t) + \sum_{i=1}^N \beta_i(t)]$. The fidelity product corresponds to $\exp[-\sum_{i=1}^N \alpha_i(t)]$, which yields $F(t) = F_P(t) \exp[\sum_{i=1}^N \beta_i(t)]$; since $\sum_{i=1}^N \beta_i(t) \geqslant 0$ we have $F(t) \geqslant F_P(t)$. Averaging over noise does not change this relation.

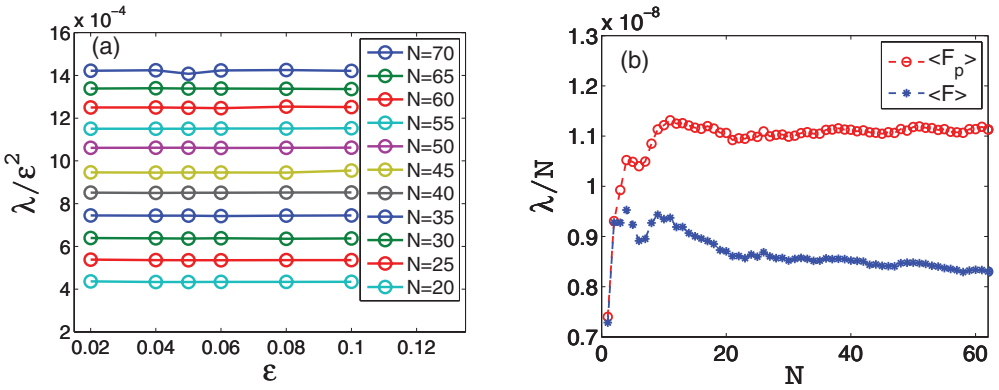


FIG. 2. (Color online) The Gaussian exponent of the fidelity as a function of ε and N. (a) The quantities $\langle\lambda\rangle/\varepsilon^2$ are plotted for different particle numbers, and they are ordered just as in the legend (higher lines are for larger values of N); obviously $\langle\lambda\rangle \propto \varepsilon^2$. (b) The quantities $\langle\lambda_P\rangle/N$ (red circles, upper line) and $\langle\lambda\rangle/N$ (blue asterisks, lower line) are plotted as a function of N for $\varepsilon = 0.05$. For larger N the lines become horizontal, indicating that $\langle\lambda\rangle \propto N \propto \langle\lambda_P\rangle$.

IV. LOSCHMIDT ECHO IN THE MEAN-FIELD REGIME

In this section we consider the Loschmidt echo in the mean-field regime, that is, by employing the Gross-Pitaevskii (GP) theory. The dynamics of Bose-Einsten condensates (BECs) is within the framework of this theory described by using the nonlinear Schrödinger equation (NLSE), which we write in dimensionless form:

$$i\frac{\partial\Phi(x,t)}{\partial t} = \left[-\frac{\partial^2}{\partial x^2} + V(x)\right]\Phi(x,t) + \tilde{g}_{1D}N|\Phi(x,t)|^2\Phi(x,t), \quad (16)$$

where $\tilde{g}_{1D} = 2mX_0g_{1D}/\hbar^2$ is the dimensionless coupling strength and $\int|\Phi(x,t)|^2dx = 1$.

To compute the fidelity of interacting BECs we repeat the same procedure as for the TG gas: first, we prepare the condensate in the ground state of the containerlike potential $V_L(x)$ (i.e., we solve numerically the stationary NLSE); second, we suddenly expand the container to $V_{2L}(x)$ and solve numerically the time-dependent NLSE in the expanded potential without noise $[V_{2L}(x)]$, and with noise $[V'_{2L}(x)]$, with identical initial conditions. This gives us $\Phi(x,t)$ and $\Phi'(x,t)$ from which we calculate the fidelity

$$F_{GP}(t) = \left|\int \Phi'^{*}(x,t)\Phi(x,t)dx\right|^2. \quad (17)$$

However, note that since we investigate the fidelity of a gas with N particles, the mean-field N-particle wave function is a product state, $\psi_{GP}(x_1,\ldots,x_N,t) = \prod_{j=1}^{N}\Phi(x_j,t)$, and therefore the N-particle mean-field fidelity is

$$F^N_{\rm GP}(t) = \left|\int \psi'^{*}_{\rm GP}\psi_{\rm GP}dx_1\cdots dx_N\right|^2 = [F_{\rm GP}(t)]^N. \quad (18)$$

Finally, we average over many different realizations of the potential to obtain $\langle F_{\rm GP}(t)\rangle_{\rm noise}$ and $\langle F^N_{\rm GP}(t)\rangle_{\rm noise}$.

In the first set of simulations, we choose the parameters in order to compare the mean-field Loschmidt echo decay to that of a TG gas. We keep all parameters identical as in Sec. III except the interaction strength, which we reduce to $\tilde{g}_{1D} = 0.04$. The number of particles is kept small ($N = 50$). The dynamics depends on the nonlinearity, defined as the product $\tilde{g}_{1D}N$. With those parameters the system is in the mean-field regime with $\gamma \approx 0.01$, and relatively small nonlinearity $\tilde{g}_{1D}N = 2$. In principle, these values can be experimentally obtained by tuning the transverse confinement frequency.

In Fig. 3(a) we plot $\langle F_{\rm GP}(t)\rangle_{\rm noise}$ and its standard deviation for noninteracting and weakly interacting BECs. We see that oscillations are superimposed on the overall decay in contrast to the TG gas case. We find that in the mean-field regime described by the Gross-Pitaevskii equation the fidelity decays faster for larger nonlinearity. It is worthy to point out that $F_{\rm GP}(t)$ is very dependent on the particular realization of $V_\varepsilon(x)$, which is not the case for the TG gas. This is illustrated in Fig. 3(b), where we show dynamics of $F_{\rm GP}(t)$ for two different realizations of the noise potential; we observe a large dependence of $F_{\rm GP}(t)$ on a particular realization of the noise. This is a consequence of the fact that the oscillation frequency of fidelity $|P_{11}(t)|^2 = \sum_{n,m}|a^1_n|^2|a^1_m|^2\cos[(\omega_n-\omega_m)t]$ for the noninteracting BEC essentially depends on the difference between only several frequencies, which is very noise sensitive, and this behavior is inherited in the nonlinear mean-field regime.

In Fig. 4 we compare the fidelities of the noninteracting BEC, the weakly interacting BEC, and the TG gas. Note that for proper comparison one should compare $F^N_{\rm GP}(t)$ with $F(t)$. We see that the mean-field fidelity shows richer behavior. In the regime of parameters we used, we find that $\langle F^N_{\rm GP}(t)\rangle_{\rm noise}$ decays faster than the TG regime fidelity in the first part of the decay dynamics, but later the mean-field regime fidelity decay slows down in comparison to the TG gas decay.

In the second set of simulations, we explore the dependence of the Loschmidt echo decay in the mean-field regime on the number of particles in the condensate, N. The dynamics of the condensate wave function $\Phi(x,t)$ in the Gross-Pitaevskii theory (16), as well as that of $F_{\rm GP}(t)$, corresponds only to the product $\tilde{g}_{1D}N$. Since the connection between $F_{\rm GP}(t)$ and $F^N_{\rm GP}(t)$ is trivial, we find it sufficient to explore the dependence of the Loschmidt echo as a function of N. For this purpose we choose the parameters to correspond to the experiments performed in Refs. [23,25]. The linear density there is much

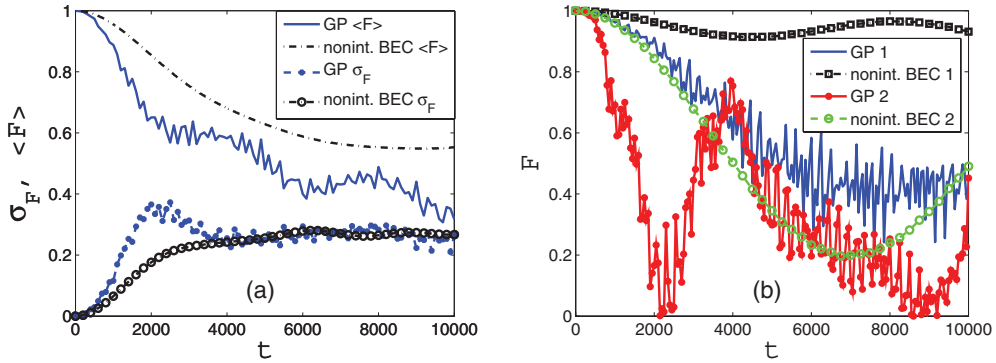


FIG. 3. (Color online) (a) Fidelities of evolving BECs for $N = 50$ and $\varepsilon = 0.05$, averaged over 50 realizations of the noise potential, and standard deviations from the noise average. The averaged fidelity for a noninteracting BEC is shown with the black dot-dashed line, and its standard deviation with open black circles. The averaged fidelity for a weakly interacting BEC is shown with the solid (blue) line, and its standard deviation with solid (blue) circles. (b) Fidelities of the evolving BECs for two different realizations of the noise potential.

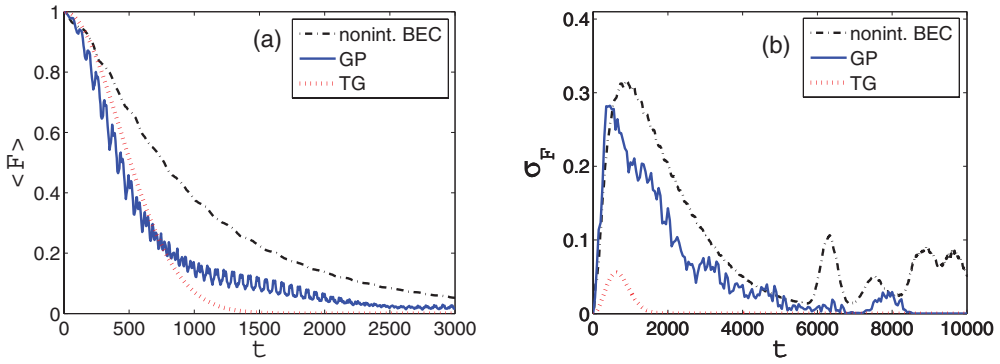


FIG. 4. (Color online) Comparison of (a) the averaged fidelities and (b) their standard deviations for the TG gas ($\langle F(t)\rangle_{\rm noise}$, red dotted line), the weakly interacting BEC ($\langle F^N_{\rm GP}(t)\rangle_{\rm noise}$, solid blue line), and the noninteracting BEC (black dot-dashed line) for the same number of particles. The parameters are $N = 50$ and $\varepsilon = 0.05$.

larger than in the TG gas case, and in the previous set of mean-field simulations. The main difference between the first and second sets of simulations in the mean-field regime is that for the first set the product $\tilde{g}_{1D}N$ is on the order of unity, whereas in the second set of simulations it is two to three orders of magnitude larger (see below). We point out that it is not reasonable to compare the mean-field results obtained with large linear densities to the TG gas case, where the linear density has to be small in order to achieve strong effective interactions [11].

From the experiment performed in Ref. [25] it follows that when the linear density of an effective 1D system is sufficiently large, its variations can affect the transverse size of the system (see also Refs. [38,39]), and the effective 1D Gross-Pitaevskii equation can be insufficient to quantitatively describe the system. In order to include these effects and check their significance we follow Ref. [38], where an effective nonpolynomial nonlinear Schrödinger equation (NPSE) was derived to take into account the transverse size effects in the dynamics of elongated cigar-shaped condensates:

$$i\frac{\partial\Phi(x,t)}{\partial t} = \left[-\frac{\partial^2}{\partial x^2} + V(x)\right]\Phi(x,t) + V_{\rm NL}(|\Phi(x,t)|^2)\Phi(x,t), \qquad (19)$$

where

$$V_{\rm NL}(|\Phi(x,t)|^2) = \tilde{g}_{1D}N\frac{|\Phi(x,t)|^2}{\sqrt{1+2a_{3D}NX_0^{-1}|\Phi(x,t)|^2}} + \frac{\hbar\omega_\perp}{2E_0}\left(\frac{1}{\sqrt{1+2a_{3D}NX_0^{-1}|\Phi(x,t)|^2}} + \sqrt{1+2a_{3D}NX_0^{-1}|\Phi(x,t)|^2}\right). \qquad (20)$$

Figure 5(a) shows the fidelity decay corresponding to $N = 1500$ and $\tilde{g}_{1D} = 0.76$ (other parameters are identical as in previous simulations), which gives $\gamma \approx 0.004$ and strong nonlinearity $\tilde{g}_{1D}N = 1140$ (these values correspond to $\omega_\perp \approx 2\pi \times 4$ kHz; see Ref. [25]). For such a large nonlinearity we recover the type of decay for $F_{\rm GP}(t)$ discovered in Ref. [33], where the Loschmidt echo is constant and close to unity for some time until it experiences an abrupt drop. Note that $F^N_{\rm GP}(t) = [F_{\rm GP}(t)]^N$ experiences this drop at a smaller value of time than $F_{\rm GP}(t)$, at values of $F_{\rm GP}(t)$ only slightly below 1, which is a consequence of large N. Let us define the times $T_{1/2}$ and $T^N_{1/2}$ at which the fidelities $F_{\rm GP}$ and $F^N_{\rm GP}$ drop to value $1/2$, respectively, via relations $F_{\rm GP}(T_{1/2}) = 1/2$ and $F^N_{\rm GP}(T^N_{1/2}) = 1/2$. The sharpness of the drop increases with

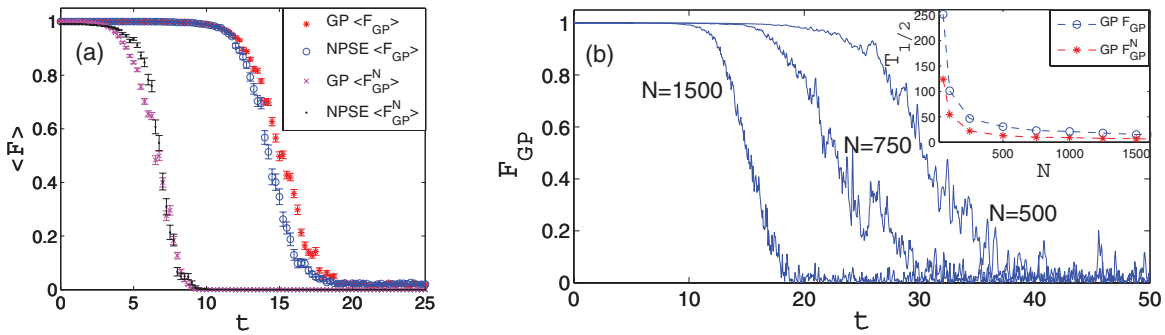


FIG. 5. (Color online) The fidelity decays in the mean-field theory obtained for large linear densities. (a) The values $\langle F_{\rm GP}(t)\rangle_{\rm noise}$ and $\langle F^N_{\rm GP}(t)\rangle_{\rm noise}$ averaged over 30 realizations of the noise potential obtained with the GP equation (16) and with the NPSE (19). Error bars correspond to the standard deviations which are smaller than in the first set of simulations [compare with Fig. 3(a)]. (b) The values of $F_{\rm GP}(t)$ for a single realization of the noise potential for $N = 500$, 750, and 1500; the inset shows the dependence of $T_{1/2}$ (blue circles) and $T^N_{1/2}$ (red asterisks) on N. See text for details.

N, and the times $T_{1/2}$ and $T_{1/2}^N$ decrease with N, as depicted in Fig. 5(b). In Figs. 5(a) and 5(b) we also compared the GP equation results with the NPSE results. We did not find a qualitative difference in the dynamics between the two models. For simulations with small linear densities presented in Fig. 3, the NPSE and the GP theory quantitatively agree.

V. DISCUSSION AND OUTLOOK

In this section we discuss the possible experiments on the Loschmidt echo dynamics for one-dimensional Bose gases. To this end, we point out that if a quasi-1D Bose system is phase-coherently split along the axial x direction, and then held for some holdup time t after which all potentials (including the transverse ones) are turned off, an interference pattern can be observed [23–25]. More specifically, the interference pattern can be used to measure the expectation value of the operator $\hat{\psi}^\dagger_{\rm right}(x,t)\hat{\psi}_{\rm left}(x,t)$ [24,26–28,30,31], and of course the quantity

$$\left\langle \int dx \hat{\psi}^\dagger_{\rm right}(x,t)\hat{\psi}_{\rm left}(x,t) \right\rangle; \tag{21}$$

here $\hat{\psi}_{\rm left,right}(x,t)$ is the bosonic field annihilation operator in the coordinate representation, where the subscripts denote the "left" and the "right" quasi-1D system (after the splitting).

Suppose that right after the splitting one of the subsystems evolves in an external potential $V_{\rm left}(x)$, and the other in a slightly perturbed potential $V_{\rm right}(x)$ for some holdup time t. These potentials could both differ from the axial potential in which the system was prepared before the splitting (for example, to take into account expansion of the trap). If the initial state of the system can be written as a superposition $\frac{1}{\sqrt{2}}[\psi_{\rm left}(x_1,\ldots,x_N,0)+\psi_{\rm right}(x_1,\ldots,x_N,0)]$, then the measurements of the interference fringes (21) correspond to the definition of the Loschmidt echo or fidelity in Eqs. (1) and (2) [with, say, $\psi_{\rm left}=\psi$ and $\psi_{\rm right}=\psi'$]. Thus, such an experimental setup can in principle be used to measure the Loschmidt echo dynamics calculated here. However, both before and after the splitting we are dealing with a single quantum system, whose state (just after the splitting) differs from the expression above. To discuss the initial conditions we consider the phase-coherent splitting in the mean-field regime separately from the splitting in the strongly interacting TG limit.

In the mean-field regime described by the Gross-Pitaevskii theory (assuming $T=0$), when the system is phase-coherently split, we have two condensates, one on the "left" and the other on the "right," in a phase-coherent state $\frac{1}{\sqrt{2}}[\Phi_{\rm left}(x,0)+\Phi_{\rm right}(x,0)]$, where $\Phi_{\rm left}$ ($\Phi_{\rm right}$) is the condensate wave function in the left (right) subsystem. Such an initial condition corresponds to our mean-field initial conditions and dynamics for some holdup time (with one of the condensates in the "noise" potential), followed by the interference measurements, corresponding to our Loschmidt echo calculations. The number fluctuations between the left and the right subsystems can for large numbers of particles be neglected.

The TG case is more complicated for several reasons. First, it seems challenging to achieve the TG gas and subsequently the splitting in the setup used in Refs. [23–25], because the system has to be extremely tight in the transverse direction, with smaller linear densities. This could be surpassed by using optical lattices where the TG gas was already achieved [11], and where splitting could be achieved by employing the technique used in Ref. [40]. Namely, by superposition of two periodic potentials, with one-half the ratio of their lattice spacing [40], and controllable intensities and relative phase, each one-dimensional tube can be split into two parallel tubes. The second complication is related to the initial state. The linear density is small, and therefore the particle number fluctuations between the left and the right subsystems should not be neglected; i.e., after the splitting the system would be in a superposition of states with different numbers of particles on the left and on the right. Furthermore, because the system is initially in the strongly correlated state, the splitting would lead to an entangled initial state, which differs from the simple superposition $\frac{1}{\sqrt{2}}(\psi_{\rm left}+\psi_{\rm right})$. In fact, if the TG state before the splitting is simply $\prod_{1\leqslant i<j\leqslant N}\mathrm{sgn}(x_i-x_j)\det_{m,n=1}^N[\psi_m(x_n)]/N!$ (we assume zero temperature), the state after the splitting can be written as

$$\psi_B(x_1,\ldots,x_N)=\frac{1}{\sqrt{N!}}\prod_{1\leqslant i<j\leqslant N}\mathrm{sgn}(x_i-x_j)\det_{m,n=1}^N \times\left\{\frac{1}{\sqrt{2}}[\psi_{m,\rm left}(x_n)+\psi_{m,\rm right}(x_n)]\right\}. \tag{22}$$

We conclude that our calculations of the Loschmidt echo performed in Sec. III do not exactly correspond to the dynamics from the initial state (22). One could conjecture that, if one of the subsystems was evolved in a potential with spatial noise, the decay of the expectation value of the operator (21) would be Gaussian in the TG regime because of the way TG states are constructed via Slater determinants and the applicability of the trace-log formula. In outlook we foresee studying dynamics from the initial state (22), which is interesting because the strong correlations of the TG state before the splitting are imprinted in this excited state.

Let us discuss several other important points. Because our calculations are performed for zero temperature, the time scale at which loss of coherence occurs due to thermal effects [23,29–31] should be sufficiently long, such that the Loschmidt echo decay due to the small random potential becomes the dominant decay mechanism. In principle this could be achieved by making the noise potential with a sufficiently large amplitude. It seems that the experiments could be made simpler by introducing two uncorrelated noise potentials in both left and right subsystems; this would not affect the type of decay observed in our simulations. Finally, let us note that the time-independent noise potential cannot realistically mimic the influence of the environment, and the thermal effects. To take into account thermal effects one should utilize a broader theoretical framework (e.g., see Refs. [29–31]).

VI. CONCLUSION

In conclusion, we have explored the Loschmidt echo (fidelity) in two regimes of one-dimensional interacting Bose gases: the strongly interacting TG regime, and the weakly

interacting mean-field regime described within the Gross-Pitaevskii theory. The gas is initially in the ground state of a trapping potential that is suddenly broadened, and the decay of fidelity is studied numerically by using a small spatial noise perturbation.

We find (numerically and analytically) that the fidelity of the TG gas decays as a Gaussian with the exponent proportional to the number of particles and the magnitude of the small perturbation squared. Our results do not depend on the details of the trapping potential; we have obtained the same behavior for a gas that is initially loaded in the ground state of the harmonic oscillator potential, which is subsequently suddenly broadened. Furthermore, we find that Gaussian decay remains if we initiate the dynamics from some excited initial state or from a superposition of such states.

In the mean-field regime the Loschmidt echo decays faster for larger nonlinearity quantified by $\tilde{g}_{1D}N$, and the decay becomes more abrupt as the nonlinearity increases (for large nonlinearities we recover the prediction made in Ref. [33]); it also shows much larger sensitivity on the particular realization of the noise, especially for small nonlinearity.

We have discussed our calculation in the context of recent experiments [23–25] and theoretical studies [26–31] on interference between parallel 1D Bose systems. We find that our calculations in the mean-field regime could be measured in such experiments. For the experiments in the TG regime, the systems using optical lattices seem to be better candidates [11]; however, the initial states that would be achieved by splitting the TG gas, and decoherence from these states, still need to be studied (see Sec. V). Finally, we would like to mention that perhaps the most interesting regime of Loschmidt echo dynamics would be for intermediate Lieb-Liniger interactions, which seem to be exactly solvable only for specific external potential configurations [41].

ACKNOWLEDGMENTS

This work is supported by the Croatian Ministry of Science (Grant No. 119-0000000-1015). H.B. acknowledges support from the Croatian-Israeli project cooperation and the Croatian National Foundation for Science. We are grateful to I. Šegota, N. Davidson, J. Goold, D. Jukić, T. Gasenzer, and R. Pezer for very useful discussions. We are grateful to the anonymous referee for suggesting us to place our work in a broader context and relate it to the already existing experiments.

[1] J. Loschmidt, Sitzungsber. Akad. Wiss. Wien II **73**, 128 (1876).
[2] L. Boltzmann, Sitzungsber. Akad. Wiss. Wien II **75**, 67 (1877).
[3] A. Peres, Phys. Rev. A **30**, 1610 (1984).
[4] R. A. Jalabert and H. M. Pastawski, Phys. Rev. Lett. **86**, 2490 (2001).
[5] Ph. Jacquod, P. G. Silvestrov, and C. W. J. Beenakker, Phys. Rev. E **64**, 055203(R) (2001)
[6] N. R. Cerruti and S. Tomsovic, Phys. Rev. Lett. **88**, 054103 (2002).
[7] T. Prosen, Phys. Rev. E **65**, 036208 (2002).
[8] T. Gorin, T. Prosen, T. H. Seligman, M. Žnidarič, Phys. Rep. **435**, 33 (2006).
[9] I. Bloch, J. Dalibard, and W. Zwerger, Rev. Mod. Phys. **80**, 885 (2008).
[10] F. Schreck, L. Khaykovich, K. L. Corwin, G. Ferrari, T. Bourdel, J. Cubizolles, and C. Salomon, Phys. Rev. Lett. **87**, 080403 (2001); A. Görlitz *et al.*, *ibid.* **87**, 130402 (2001); M. Greiner, I. Bloch, O. Mandel, T. W. Hänsch, and T. Esslinger, *ibid.* **87**, 160405 (2001); H. Moritz, T. Stöferle, M. Kohl, and T. Esslinger, *ibid.* **91**, 250402 (2003); B. Laburthe-Tolra, K. M. O'Hara, J. H. Huckans, W. D. Phillips, S. L. Rolston, and J. V. Porto, *ibid.* **92**, 190401 (2004); T. Stöferle, H. Moritz, C. Schori, M. Kohl, and T. Esslinger, *ibid.* **92**, 130403 (2004).
[11] T. Kinoshita, T. Wenger, and D. S. Weiss, Science **305**, 1125 (2004); B. Paredes, A. Widera, V. Murg, O. Mandel, S. Fölling, I. Cirac, G. V. Shlyapnikov, T. W. Hänsch, and I. Bloch, Nature (London) **429**, 277 (2004).
[12] T. Kinoshita, T. Wenger, and D. S. Weiss, Nature (London) **440**, 900 (2006).
[13] M. Olshanii, Phys. Rev. Lett. **81**, 938 (1998).
[14] E. Lieb and W. Liniger, Phys. Rev. **130**, 1605 (1963); E. Lieb, *ibid.* **130**, 1616 (1963).
[15] M. Girardeau, J. Math. Phys. **1**, 516 (1960).
[16] M. D. Girardeau and E. M. Wright, Phys. Rev. Lett. **84**, 5691 (2000).
[17] M. Rigol and A. Muramatsu, Phys. Rev. Lett. **94**, 240403 (2005).
[18] A. Minguzzi and D. M. Gangardt, Phys. Rev. Lett. **94**, 240404 (2005).
[19] M. Rigol, V. Dunjko, V. Yurovsky, and M. Olshanii, Phys. Rev. Lett. **98**, 050405 (2007).
[20] A. del Campo and J. G. Muga, Europhys. Lett. **74**, 965 (2006).
[21] R. Pezer and H. Buljan, Phys. Rev. Lett. **98**, 240403 (2007).
[22] M. F. Andersen, A. Kaplan, T. Grünzweig, and N. Davidson, Phys. Rev. Lett. **97**, 104102 (2006).
[23] S. Hofferberth, I. Lesanovsky, B. Fischer, T. Schumm, and J. Schmiedmayer, Nature (London) **449**, 324 (2007).
[24] S. Hofferberth, I. Lesanovsky, B. Fischer, T. Schumm, and J. Schmiedmayer, Nat. Phys. **4**, 489 (2008).
[25] P. Krüger, S. Hofferberth, I. E. Mazets, I. Lesanovsky, and J. Schmiedmayer, Phys. Rev. Lett. **105**, 265302 (2010).
[26] A. Polkovnikov, E. Altman, and E. Demler, Proc. Natl. Acad. Sci. USA **103**, 6125 (2006).
[27] V. Gritsev, E. Altman, E. Demler, and A. Polkovnikov, Nat. Phys. **2**, 705 (2006).
[28] R. Bistritzer and E. Altman, Proc. Natl. Acad. Sci. USA **104**, 9955 (2007).
[29] A. A. Burkov, M. D. Lukin, and E. Demler, Phys. Rev. Lett. **98**, 200404 (2007).
[30] I. E. Mazets and J. Schmiedmayer, Eur. Phys. J. B **68**, 335 (2009).
[31] H.-P. Stimming, N. J. Mauser, J. Schmiedmayer, and I. E. Mazets, Phys. Rev. A **83**, 023618 (2011).

[32] J. Billy, V. Josse, Z. Zuo, A. Bernard, B. Hambrecht, P. Lugan, D. Clement, L. Sanchez-Palencia, P. Bouyer, and A. Aspect, Nature (London) **453**, 891 (2008).
[33] G. Manfredi and P.-A. Hervieux, Phys. Rev. Lett. **100**, 050405 (2008).
[34] J. Martin, B. Georgeot, and D. L. Shepelyansky, Phys. Rev. Lett. **101**, 074102 (2008).
[35] J. Goold, T. Fogarty, M. Paternostro, and Th. Busch, e-print arXiv:1104.2577v1.
[36] A. del Campo, Phys. Rev. A **84**, 012113 (2011).
[37] L. Benet, S. Hernandez-Quiroz, and T. H. Seligman, Phys. Rev. E **83**, 056216 (2011).
[38] L. Salasnich, A. Parola, and L. Reatto, Phys. Rev. A **65**, 043614 (2002).
[39] F. Gerbier, Europhys. Lett. **66**, 771 (2004).
[40] S. Fölling, S. Trotzky, P. Cheinet, M. Feld, R. Saers, A. Widera, T. Müller, and I. Bloch, Nature (London) **448**, 1029 (2007).
[41] H. Buljan, R. Pezer, and T. Gasenzer, Phys. Rev. Lett. **100**, 080406 (2008); **102**, 049903(E) (2009); D. Jukić, R. Pezer, T. Gasenzer, and H. Buljan, Phys. Rev. A **78**, 053602 (2008); D. Jukić and H. Buljan, New J. Phys. **12**, 055010 (2010); D. Jukić, S. Galić, R. Pezer, and H. Buljan, Phys. Rev. A **82**, 023606 (2010).